Josephson tunnelling involving superconductors with charge-density waves

1997 J. Phys.: Condens. Matter 9 3901

(http://iopscience.iop.org/0953-8984/9/19/011)

J. Phys.: Condens. Matter **9** (1997) 3901–3920. Printed in the UK PII: S0953-8984(97)76628-1

Josephson tunnelling involving superconductors with charge-density waves

Alexander M Gabovich and Alexander I Voitenko

Crystal Physics Department, Institute of Physics, National Academy of Sciences, 252650 Kiev-22 GSP, Prospekt Nauki 46, Ukraine†

Received 24 July 1996, in final form 10 February 1997

Abstract. The non-stationary Josephson (I^1-), and quasiparticle (J-) currents through symmetrical and non-symmetrical tunnel junctions involving superconductors with charge-density waves were calculated. In both cases the voltage dependences of the currents have logarithmic singularities and jumps at positions determined by the non-trivial combinations of the superconducting, Δ, and dielectric, Σ, order parameters. The current J in non-symmetrical junctions is an asymmetrical function of the voltage, and depends on the sign of Σ. For symmetrical junctions this current may be either symmetrical or not, depending on the relationship between the signs of the Σs on either side of the junction.

1. Introduction

The superconducting coherent state was long ago recognized as a state with so-called off-diagonal long-range order (ODLRO), this concept being closely connected with the existence of Gor'kov's anomalous Green's functions $\mathbf{F}(\boldsymbol{p}, \omega_n)$ [1]. Here $\omega_n = (2n+1)\pi T, n = 0, \pm 1, \pm 2, \ldots, T$ is the temperature, $\hbar = k_B = 1$, and $\hbar$ and k_B are Planck's and Boltzmann's constants respectively. On the other hand, for the primordial electron spectra of metals involving congruent (nested) Fermi surface (FS) sections, the electron–hole correlations below some critical temperature T_d can lead to the existence of a distorted state [2, 3] which corresponds to diagonal long-range order (DLRO), and can appear due to electron–phonon or Coulomb interactions. In particular, electron–hole attraction may result in the appearance of the so-called excitonic insulator state of condensed matter, which separates semiconducting and semimetallic phases at low T. The excitonic state has been recently discovered in certain rare-earth compounds [4]. Four types of DLRO are possible, according to the properties of the order parameter in the low-T phase [2]. But only two of them have been realized so far in experiment: charge-density waves (CDWs) [5, 6] induced by spin-singlet electron–hole pairing, and spin-density waves (SDWs) [7] induced by spin-triplet antiferromagnetic pairing. The transport properties of the 'dielectrized' distorted phase depend on the degree of FS gapping: if the gapping is complete, the substance becomes an insulator below T_d; otherwise it remains metallic but with lower conductivity. Coexistence of DLRO and superconducting ODLRO in the case of partial 'dielectrization' has been observed for many classes of materials [5, 8, 9]. For instance, there is experimental and theoretical evidence for the existence of CDWs in the superconducting state of high-T_c oxides [10]. For example, electron diffraction measurements [11] revealed

† E-mail address: collphen@marion.iop.kiev.ua.

0953-8984/97/193901+20$19.50

CDW existence below $T_d = 69$ K in the low-temperature tetragonal (LTT) phase of $La_{1.875}Ba_{0.125}CuO_4$, and below $T_d = 104$ K in the *pccn* state of the orthorhombic system of $La_{1.885}Sr_{0.115}CuO_4$. For $La_{1.880-y}Nd_ySr_{0.120}CuO_4$ CDWs were found in the *pccn* phase which is stable when $T < T_{d1} \approx 100$ K, as well as for the LTT phase emerging in the range $T_{d1} < T < T_{d2} \approx 150$ K. CDWs have also been observed by the scanning tunnelling microscopy (STM) technique in $YBa_2Cu_3O_{7-y}$ [12].

In this connection, one should also mention the popular scenario [13] of atom rearrangement caused by the electron–phonon interaction due to a Van Hove singularity of the electron density of states inherent to two-dimensional structures. This mechanism of structural instability is, however, not universal. That is, it may be realized in highly anisotropic substances, e.g., in 214 and 123 superconductors, but not in distorted cubic solid solutions generated from $BaBiO_3$. Nevertheless, the Van Hove singularity approach can be regarded as a semi-microscopical justification for the considerations presented in this article.

We use here the simple Bilbro–McMillan model [14] of the phase coexistence where only a nested part of the FS is 'dielectrized' for $T < T_d$. At the same time, the superconducting isotropic gap Δ emerges for the whole FS for $T < T_c$, and the Fermi level lies *inside* the dielectric gap region. The theory of CDW superconductivity [8–10, 15] based on the model introduced in [14] made it possible to explain many superconducting and normal-state properties of structurally unstable substances. Given partially 'dielectrized' superconductors, it is natural to assume that the emerging CDW severely affects the tunnelling of normal electrons and Cooper pairs. The dependences of the stationary critical Josephson current I_c on T, the dielectric gap magnitude, and the nested fraction of the FS have been obtained in [16]. It turned out that the normalized function $I_c(T)/I_c(0)$ versus T/T_c does not differ substantially from the classical Ambegaokar–Baratoff curve [17]. At the same time, the amplitude of $I_c(T)$ is strongly reduced with the increase of the nested FS fraction and the magnitude of the dielectric gap.

In this paper we investigate the more involved case of the non-stationary Josephson effect in tunnel junctions with one or both electrodes being CDW superconductors. The amplitudes of the Josephson (I^1-), pair–quasiparticle interference (I^2-), and quasiparticle (J-) currents through tunnel junctions are calculated.

2. Partially 'dielectrized' superconductors

The model Hamiltonian of the partially gapped (partially 'dielectrized') CDW superconductor has the form [14, 18]

$$\mathcal{H} = \mathcal{H}_0 + \mathcal{H}_{\mathrm{MF}}. \tag{1}$$

Here

$$\mathcal{H}_0 = \sum_{i=1}^{3} \sum_{p\alpha} \xi_i(\boldsymbol{p})\, a^{\dagger}_{ip\alpha}\, a_{ip\alpha} \tag{2}$$

is the free-electron Hamiltonian. The operator $a^{\dagger}_{ip\alpha}$ ($a_{ip\alpha}$) is the creation (annihilation) operator of a quasiparticle with a quasimomentum $\boldsymbol{p}$ and spin projection α from the ith FS section. The summation index i denotes different FS sections. That is, $i = 1$ and $i = 2$ for the nested sections where the electron spectrum is degenerate:

$$\xi_1(\boldsymbol{p}) = -\xi_2(\boldsymbol{p} + \boldsymbol{Q}) \tag{3}$$

where $\boldsymbol{Q}$ is the CDW vector, while $i = 3$ for the rest of the FS, where the dispersion relation for elementary excitations is described by the different function $\xi_3(\boldsymbol{p})$.

The mean-field term $\mathcal{H}_{\mathrm{MF}}$ in the Hamiltonian (1)

$$\mathcal{H}_{\mathrm{MF}} = \mathcal{H}_{\mathrm{BCS}} + \mathcal{H}_{\mathrm{CDW}} \tag{4}$$

is the sum of the BCS term

$$\mathcal{H}_{\mathrm{BCS}} = -\Delta \sum_{i=1}^{3} \sum_{\boldsymbol{p}} a^{\dagger}_{i\boldsymbol{p}\uparrow}\, a^{\dagger}_{i,-\boldsymbol{p},\downarrow} + \mathrm{HC} \tag{5}$$

which is responsible for the superconductivity, and the CDW term

$$\mathcal{H}_{\mathrm{CDW}} = -\Sigma \sum_{i=1}^{2} \sum_{\boldsymbol{p}\alpha} a^{\dagger}_{i\boldsymbol{p}\alpha}\, a_{i,\boldsymbol{p}+\boldsymbol{Q},\alpha} + \mathrm{HC} \tag{6}$$

describing the electron–hole excitonic pairing. It is sufficient [19] to use the mean-field simplified version (5) of the original BCS Hamiltonian [1], because all of the correlation effects are neglected here from the very beginning. On the other hand, the mean-field term (6) replaces the sum of the Coulomb electron–hole attraction [2, 3] and the electron–phonon interband interaction [3], thus describing the excitonic insulator and the Peierls insulator simultaneously (see also references [15, 20–22]). The effective interaction matrix element which is responsible for the excitonic (Peierls) pairing determines the dielectric order parameter Σ implicitly, the approach based on equation (6) becoming phenomenological.

The dielectric order parameter Σ emerges on the nested FS sections, so the summation in equation (6) is carried out over them only. In contrast, the superconducting order parameter Δ appears over the entire FS. We should stress that the existence of a *single* Δ for the multisectional FS is the consequence of a strong mixing between different branches of the electron spectrum, when all matrix elements of the four-pole electron–electron interaction are assumed to be equal [14, 15, 21]. In this case, the effective coupling constants for Δ and Σ are different [21, 20], so they can be considered as independent phenomenological functions of T and their forms and magnitudes are to be extracted from experiment.

If the mixing is of intermediate strength, there are equal superconducting order parameters, $\Delta_1 = \Delta_2$, on the nested FS sections, and a dissimilar one, Δ_3, on the non-degenerate FS section [20]. At the same time, the Cooper pairing of quasiparticles from the sections 1 or 2, on the one hand, and their counterparts, on the other hand, is not essential, because the sections are non-congruent and the corresponding interaction matrix elements are small. In the framework of this approach, a multiple-component order parameter has been recently proposed [23] for high-T_c oxides using the anisotropic tight-binding approximation for the electron spectrum in order to explain the photoelectron data, revealing the superconducting gap anisotropy [24, 25]. For the problem studied here, such a generalization can only lead to much more cumbersome expressions, but the main features found below will remain unaltered. However, the concept of different coexisting Δ_i may be in doubt *per se* for dirty superconductors such as oxide ceramics, due to the impurity isotropization of the superconducting order parameter [1, 26]. That is why only the limiting case of strong mixing with a single Δ is considered here.

The order parameter Σ in equation (6) is real with either sign. For each sign the shape of the current–voltage characteristic (CVC) for tunnel junctions is different [18, 27, 28]. On the other hand, the stationary Josephson current [16] and the thermodynamic quantities for partially 'dielectrized' superconductors [15] do not depend on the sign of Σ. The temperature dependence of Σ is generally unknown. At the same time, for all actual CDW superconducting substances discussed here, the inequality $T_d > T_c$ (or even $T_d \gg T_c$) holds.

Therefore, the exact form of the function $\Sigma(T)$ is not crucial for the determination of the $\Delta(T)$ dependence. Moreover, the calculations of Bilbro and McMillan [14] showed that below T_c the superconducting gap Δ stabilizes the magnitude of Σ at a certain constant level. Taking into account the above-mentioned circumstances, we did not perform self-consistent calculations of $\Delta(T)$ and $\Sigma(T)$ in this paper. Instead, we suggested for $\Sigma(T)$ either a trivial constant behaviour or a BCS behaviour, the latter inherent to the basic mean-field excitonic [3] or Peierls [5] scenarios.

The normal $\mathbf{G}_{ij}^{\alpha\beta}(\boldsymbol{p};\omega_n)$ and anomalous $\mathbf{F}_{ij}^{\alpha\beta}(\boldsymbol{p};\omega_n)$ Matsubara Green's functions corresponding to the Hamiltonian (1) can be found from the Dyson–Gor'kov equations obtained earlier. They are matrices in the space which is the direct product of the spin space and the isotopic space of the FS sections [15]. If one makes allowance for the matrix structure of the order parameters which is implicitly contained in equations (5) and (6), the following expressions can be obtained:

$$\mathbf{G}_{nd}(\boldsymbol{p};\omega_n) = -\frac{\mathrm{i}\omega_n + \xi_3(\boldsymbol{p})}{\omega_n^2 + \Delta^2 + \xi_3^2(\boldsymbol{p})} \tag{7}$$

$$\mathbf{F}_{nd}(\boldsymbol{p};\omega_n) = \frac{\Delta}{\omega_n^2 + \Delta^2 + \xi_3^2(\boldsymbol{p})} \tag{8}$$

$$\mathbf{G}_{d}(\boldsymbol{p};\omega_n) = -\frac{\mathrm{i}\omega_n + \xi_1(\boldsymbol{p})}{\omega_n^2 + \Delta^2 + \Sigma^2 + \xi_1^2(\boldsymbol{p})} \tag{9}$$

$$\mathbf{F}_{d}(\boldsymbol{p};\omega_n) = \frac{\Delta}{\omega_n^2 + \Delta^2 + \Sigma^2 + \xi_1^2(\boldsymbol{p})} \tag{10}$$

$$\mathbf{G}_{is}(\boldsymbol{p};\omega_n) = -\frac{\Sigma}{\omega_n^2 + \Delta^2 + \Sigma^2 + \xi_1^2(\boldsymbol{p})}. \tag{11}$$

Here the subscript *nd* corresponds to the 'non-dielectrized' part 3 of the FS, *d* to the nested ('dielectrized') parts 1 and 2, and *is* to the intersection excitonic (electron–hole) pairing between the quasiparticle from part 1 and the $\boldsymbol{Q}$-shifted quasiparticle from part 2. We note that the Green's function $\mathbf{F}_{is}$ is identically zero for CDW superconductors.

3. Tunnel currents

To calculate the total tunnel current I through the junction we employ the conventional approach [17, 29] based on the junction Hamiltonian

$$\mathcal{H}_{\mathrm{jun}} = \mathcal{H} + \mathcal{H}' + \mathcal{T}. \tag{12}$$

The left- and right-hand-side electrodes of the junction are described in equation (12) by the terms $\mathcal{H}$ and $\mathcal{H}'$, respectively, which coincide with the Hamiltonian (1) with an accuracy of notations. Hereafter primed entities including subscripts and superscripts correspond to the right-hand side of the junction. The tunnel term $\mathcal{T}$ has the form

$$\mathcal{T} = \sum_{i,i'=1}^{3} \sum_{\boldsymbol{p}\boldsymbol{q}'\alpha} \mathbf{T}_{\boldsymbol{p}\boldsymbol{q}'}^{ii'} a_{i\boldsymbol{p}\alpha}^{\dagger} a_{i'\boldsymbol{q}'\alpha} + \mathrm{HC} \tag{13}$$

where the $\mathbf{T}_{\boldsymbol{p}\boldsymbol{q}'}^{ii'}$ are the tunnel matrix elements. The general expression for $I(T)$ obtained in the second order of the perturbation theory in $\mathcal{T}$ is a sum of terms:

$$I_{iji'j'} \propto \sum_{\boldsymbol{p}\boldsymbol{q}'} \mathbf{T}_{\boldsymbol{p}\boldsymbol{q}'}^{ii'} \mathbf{T}_{\boldsymbol{p}\boldsymbol{q}'}^{jj'*} \int_{-\infty}^{\tau} \mathrm{d}\tau_1 \, \{F_{ij}^{*}(\boldsymbol{p}, \tau - \tau_1) F_{i'j'}^{+*}(\boldsymbol{q}', \tau - \tau_1)$$

$$- F_{ij}^{+}(\boldsymbol{p},\tau-\tau_1)F_{i'j'}(\boldsymbol{q}',\tau-\tau_1)+G_{ij}(\boldsymbol{p},\tau-\tau_1)G_{i'j'}(\boldsymbol{q}',\tau-\tau_1)$$
$$- G_{ij}^{*}(\boldsymbol{p},\tau-\tau_1)G_{i'j'}^{*}(\boldsymbol{q}',\tau-\tau_1)\} \tag{14}$$

where $F(\boldsymbol{p},\tau)$ and $G(\boldsymbol{p},\tau)$ are temporal Green's functions, and the asterisk denotes complex conjugation.

We assume that all matrix elements $\mathbf{T}^{ii'}$ are equal and not influenced by the existence of the superconducting and dielectric gaps, so that

$$\mathbf{T}^{ii'}\mathbf{T}^{jj'*}=\text{constant}=|\mathbf{T}|^2. \tag{15}$$

This approximation is analogous to the neglect of the influence of the gap Δ on $|\mathbf{T}|^2$ in the standard Ambegaokar–Baratoff approach [17]. Our assumption is natural in the framework of the BCS-type scheme, i.e., in the case of a weak coupling for Cooper and zero-channel pairings. The weak-coupling approach is valid for the latter if the inequality $E_{\mathrm{F}}\gg\Sigma$ holds, where E_{F} is the Fermi energy. Then we can introduce the universal tunnel resistance R:

$$R^{-1}=4\pi e^2N(0)N'(0)\langle|\mathbf{T}|^2\rangle_{\mathrm{FS}} \tag{16}$$

where $N(0)$ and $N'(0)$ are the total electron densities of states for left- and right-hand-side metals. They are the sums of the densities of states for 'dielectrized' and 'non-dielectrized' parts of the FS. For example, $N(0)=N_d(0)+N_{nd}(0)$. The ratio

$$\nu=N_{nd}(0)/N_d(0) \tag{17}$$

characterizes the degree of 'dielectrization' of the metal. A similar parameter ν' can be introduced also for right-hand-side metal. Angle brackets $\langle\cdots\rangle_{\mathrm{FS}}$ in equation (16) imply averaging over the FS. In performing such an averaging it is assumed that the Fermi momentum k_{F} is the same for d- and nd-FS sections for each superconductor [14, 15].

One should bear in mind that it is the set of Green's functions (7)–(11) that makes a contribution when calculating the tunnel current I across the junction. Then for the case when an ac voltage $V(\tau)\equiv V_{\mathrm{right}}(\tau)-V_{\mathrm{left}}(\tau)$ across the Josephson junction varies adiabatically slowly as compared with the energies of the order of T_c, i.e., $V^{-1}\,\mathrm{d}V/\mathrm{d}\tau\ll T_c$, and taking into account the symmetry of the problem, we obtain expressions which are generalizations of those for the BCS superconductors [29]:

$$I[V(\tau)]=\sum_{i=1}^{4}[I_i^1(V)\sin 2\phi+I_i^2(V)\cos 2\phi]+\sum_{i=1}^{9}J_i(V)\equiv\sum_{i=1}^{4}I_i(V)+\sum_{i=1}^{9}J_i(V) \tag{18}$$

where $\phi=\int^{\tau}eV(\tau)\,\mathrm{d}\tau$. Here $I^1=\sum_{i=1}^{4}I_i^1$ is the Josephson current, $I^2=\sum_{i=1}^{4}I_i^2$ is the pair–quasiparticle interference current, and $J=\sum_{i=1}^{9}J_i$ is the quasiparticle current. The quantities $I_i^{1,2}$ and J_i are functionals of the Green's functions $F_{ij}(\omega)$ and $G_{ij}(\omega)$, which are in turn the Fourier transforms of the time-dependent Green's functions $F_{ij}(\boldsymbol{p},\tau)$ and $G_{ij}(\boldsymbol{p},\tau)$ from equation (14), integrated over $\boldsymbol{p}$. The explicit expressions for $I_i^{1,2}$ and J_i are given in appendix A.

When obtaining equation (18), we made an implicit suggestion of strong pinning of the CDWs (e.g., by impurities or the host crystal lattice), so their phases χ_1 and χ_2 on either side of the junction are fixed. At the same time, in the framework of the fundamental generic models of the dielectric pairing, e.g., for the Peierls insulator [5], the phase of the CDW (and consequently the phase χ of the order parameter $\Sigma\equiv|\Sigma|\exp(\mathrm{i}\chi)$) is arbitrary. This fact leads, in particular, to the Fröhlich sliding-wave conductivity [5, 30].

Pinning prevents sliding in Peierls quasi-one-dimensional compounds for small electric fields, whereas for large fields various coherent phenomena of the Josephson type become possible. For excitonic insulators produced by the combined action of the Coulomb and

electron–phonon interactions, and thus being more adequate approximations to the real substances, the behaviour is more involved. In particular, the phase is fixed by Coulomb interband matrix elements (linking FS sections 1 and 2) corresponding to two-particle transitions V_2, and the interband electron–phonon interaction determined by the constant λ_{e-ph} [2, 3, 31, 32]. Moreover, the excitonic transitions due to the finite values of V_2 and λ_{e-ph} are always of the first order although close to the second-order transitions [32, 33]. The contributions from single-particle Coulomb interband matrix elements V_3, which connect three particles from, say, FS section 1 and one particle from FS section 2, or vice versa, result in even more radical consequences. Namely, the self-consistency equation for the order parameter Σ becomes non-homogeneous, with the right-hand side proportional to V_3. This leads to the fixing of the phase χ [22]. A similar equation was obtained earlier for the semiconductor band gap in strong electromagnetic fields [34].

A consideration of the quasiparticle tunnel current $J(V)$ between two Peierls insulators with free phases χ_1 and χ_2 in the absence of superconductivity and for complete 'dielectrization' was carried out in reference [35], whereas in the case of fixed χ_1 and χ_2, and partial 'dielectrization', $J(V)$ was calculated by the present authors [18]. An attempt to generalize the results [35], taking into account the finite strength of the insulating barrier potential at the interface in the spirit of the model given in [36] for superconductors has been recently made in reference [37]. However, the final expressions for currents in references [35, 37] are quite different, and in addition the treatment in [37] does not include erroneously the contribution of the Andreev-like [38] reflection, for which allowance should be made in CDW-based junctions [39].

4. Current–voltage characteristics

The equations of appendix A can be simplified for two important particular cases: (i) the symmetrical S–I–S case in which the CDW superconductors (S) to the left and to the right of the interlayer (I) are identical; and (ii) the non-symmetrical case S–I–S_{BCS} in which one of the electrodes is an ordinary BCS superconductor (S_{BCS}) or a normal metal (of course, in the latter situation, only the quasiparticle current J remains).

For the symmetrical junction $\nu' = \nu$, and the number of independent Green's functions is reduced substantially:

$$\begin{aligned} &F_{11} = F'_{11} \equiv F_d \qquad F_{33} = F'_{33} \equiv F_{nd} \\ &G_{11} = G'_{11} \equiv G_d \qquad G_{12} = G'_{12} \equiv G_{is} \qquad G_{33} = G'_{33} \equiv G_{nd}. \end{aligned} \tag{19}$$

Then equation (18) can be rewritten as

$$I_s = \sum_{i=1}^{3} I_{si}(V) + \sum_{i=1}^{4} J_{si}(V) \tag{20}$$

where

$$\begin{aligned} &I_{s1} = I_1 \qquad I_{s2} = I_2 + I_3 \qquad I_{s3} = I_4 \\ &J_{s1} = J_1 \qquad J_{s2} = J_4 \qquad J_{s3} = J_5 + J_7 \qquad J_{s4} = J_9. \end{aligned} \tag{21}$$

The currents J_2 and J_3 as well as J_6 and J_8 compensate each other.

In the non-symmetrical case, $N'_d(0) = 0$, so, according to equation (17), $\nu' = \infty$. Only the following Green's functions are inherent to this junction:

$$\begin{aligned} &F_{11} \equiv F_d \qquad F_{33} \equiv F_{nd} \qquad F'_{33} \equiv F' \\ &G_{11} \equiv G_d \qquad G_{12} \equiv G_{is} \qquad G_{33} \equiv G_{nd} \qquad G'_{33} \equiv G'. \end{aligned} \tag{22}$$

Here F' and G' are the Green's functions of the BCS superconductor which can be formally obtained from F_{nd} and G_{nd} with the BCS order parameter $\Delta_{\mathrm{BCS}}(T)$ substituted for $\Delta(T)$. Then the total current through the junction considered is

$$I_{ns} = \sum_{i=1}^{2} I_{nsi}(V) + \sum_{i=1}^{3} J_{nsi}(V) \tag{23}$$

where

$$\begin{aligned} &I_{ns1} = I_2 \qquad I_{ns2} = I_4 \\ &J_{ns1} = J_5 \qquad J_{ns2} = J_6 \qquad J_{ns3} = J_9. \end{aligned} \tag{24}$$

If the right-hand-side electrode is normal metal, $\Delta_{\mathrm{BCS}} \equiv 0$, and as a consequence $F' \equiv 0$ and $I_{nsi}(V) \equiv 0$.

The Green's functions (19) and (22) are related to their Matsubara counterparts (7)–(11) in the following manner. First, the thermal functions $\mathbf{F}_{d,nd}(\boldsymbol{p};\omega_n)$ and $\mathbf{G}_{d,nd,is}(\boldsymbol{p};\omega_n)$ are integrated over the momentum $\boldsymbol{p}$, and the analytical continuation is made to the real axis of the variable $\mathrm{i}\omega_n$ [1]. The result is

$$\mathbf{G}^R_{nd}(\omega) = -\frac{\pi\omega}{\sqrt{\Delta^2 - (\omega + \mathrm{i}0)^2}} \tag{25}$$

$$\tilde{\mathbf{F}}_{nd}(-\mathrm{i}\omega) = \frac{\pi\Delta}{\sqrt{\Delta^2 - (\omega + \mathrm{i}0)^2}} \tag{26}$$

$$\mathbf{G}^R_{d}(\omega) = -\frac{\pi\omega}{\sqrt{D^2 - (\omega + \mathrm{i}0)^2}} \tag{27}$$

$$\tilde{\mathbf{F}}_{d}(-\mathrm{i}\omega) = \frac{\pi\Delta}{\sqrt{D^2 - (\omega + \mathrm{i}0)^2}} \tag{28}$$

$$\mathbf{G}^R_{is}(\omega) = -\frac{\pi\Sigma}{\sqrt{D^2 - (\omega + \mathrm{i}0)^2}}. \tag{29}$$

Here $D = (\Delta^2 + \Sigma^2)^{1/2}$ and the superscript R reflects the retarded character of the Green's functions. The respective functions for the right-hand-side superconductor $(\mathbf{G}^R)'(\omega)$ and $\tilde{\mathbf{F}}'(-\mathrm{i}\omega)$ can be obtained from $\mathbf{G}^R_{nd}(\omega)$ and $\tilde{\mathbf{F}}_{nd}(-\mathrm{i}\omega)$ with $\Delta(T)$ replaced by $\Delta_{\mathrm{BCS}}(T)$. Second, the functions (25)–(29) are connected to the temporal Green's functions from equations given in appendix A by the dispersion relations [1, 29]

$$G(\omega) = \mathrm{Re}\,\mathbf{G}^R(\omega) + \mathrm{i}\tanh\frac{\omega}{2T}\,\mathrm{Im}\,\mathbf{G}^R(\omega) \tag{30}$$

$$\mathrm{i}F^+(\omega) = -\mathrm{i}F(\omega) = \mathrm{Re}\,\tilde{\mathbf{F}}(-\mathrm{i}\omega) + \mathrm{i}\tanh\frac{\omega}{2T}\,\mathrm{Im}\,\tilde{\mathbf{F}}(-\mathrm{i}\omega). \tag{31}$$

The resulting expressions for all possible currents are presented in appendix B.

5. Results of calculations

As is well known [17, 29, 40], the CVC $I^{1,2}(V)$ and $J(V)$ for ordinary BCS superconductors possess logarithmic singularities (the so-called Riedel peaks) and discontinuities at certain voltages V. The characters and magnitudes of the singularities for different kinds of current are correlated due to the existence of the Kramers–Kronig relationships between them [40]. In our case of the CDW superconductors, the dependences $I^{1,2}(V)$ and $J(V)$ are much more involved than the respective curves in the conventional case owing to the existence of two energy gaps ($|\Sigma|$ and Δ) instead of one (Δ), and their interplay. All of the current

components for symmetrical and non-symmetrical cases can be calculated analytically for $T = 0$. The cumbersome expressions obtained are analogous to the results in the framework of the BCS theory and will be presented elsewhere. When $T \neq 0$ the CVC can be calculated only numerically. But the characteristic features can be found for arbitrary temperatures. Below we present relevant formulas only for the Josephson and quasiparticle currents. The types of peculiarity for the interference current are identical to those of the latter.

For symmetrical S–I–S junctions the usual symmetry relations

$$I_s^1(-V) = I_s^1(V) \qquad J_s(-V) = -J_s(V) \tag{32}$$

hold, and the CVC do not depend on the sign of Σ. So, for definiteness, let $V > 0$.

The Riedel singularities of the Josephson current $I_s^1(V)$ are defined by the feature points of its components

$$I_{s1}^1(eV \approx 2D) \approx \frac{1}{eR(1+\nu)^2}\frac{\Delta^2}{4D}W_1(D, D) \tag{33}$$

$$I_{s2}^1(eV \approx D + \Delta) \approx \frac{\nu}{2eR(1+\nu)^2}\sqrt{\frac{\Delta^3}{D}}W_1(D, \Delta) \tag{34}$$

$$I_{s3}^1(eV \approx 2\Delta) \approx \frac{\nu^2\Delta}{4eR(1+\nu)^2}W_1(\Delta, \Delta) \tag{35}$$

where the following notation was used:

$$W_1(\Delta_1, \Delta_2) = \left(\tanh\frac{\Delta_1}{2T} + \tanh\frac{\Delta_2}{2T}\right)\ln\frac{\Delta_1 + \Delta_2}{|eV - (\Delta_1 + \Delta_2)|}. \tag{36}$$

Among this family of singularities, only the latter can be found in the BCS case ($\nu \to \infty$). Two others are inherent to CDW superconductors and vanish when the dielectric gapping is absent.

At finite temperatures a new feature of Josephson currents appears:

$$\delta I_{s2}^1(eV = D - \Delta) = \frac{\pi\nu}{2eR(1+\nu)^2}\sqrt{\frac{\Delta^3}{D}}\left(\tanh\frac{D}{2T} - \tanh\frac{\Delta}{2T}\right). \tag{37}$$

Here the notation $\delta I(eV = x) \equiv I(eV = x + 0) - I(eV = x - 0)$ was introduced. One should note that this peculiarity is inherent to *non-symmetrical* junctions with BCS superconductors [40], whereas in our case it can be observed also for *symmetrical* ones. The origin of this feature is the existence of two kinds of FS section with different effective gaps, namely, D and Δ. Thus, Cooper pair or single-electron tunnelling between the 'dielectrized' FS section of one electrode and the 'non-dielectrized' section of another one occurs as if the junction is asymmetric. Of course, the peculiarity at $|eV| = D - \Delta$ diminishes when $T \to 0$ due to the lack of the thermally induced quasiparticles below and above the gaps, and disappears at $T = 0$. So, a useful test is proposed for checking the possible coexistence of the order parameters Δ and Σ when other methods give uncertain results.

The CVC for the quasiparticle tunnel current $J_s(V)$ also changes considerably due to the partial 'dielectrization' of the electron spectrum. That is, the following discontinuities emerge:

$$\delta J_{s1}(eV = 2D) = \frac{\pi D}{2eR(1+\nu)^2}\tanh\frac{D}{2T} \tag{38}$$

$$\delta J_{s2}(eV = 2D) = -\frac{\pi}{2eR(1+\nu)^2}\frac{\Sigma^2}{D}\tanh\frac{D}{2T} \tag{39}$$

$$\delta J_{s3}(eV = D + \Delta) = \frac{\pi\nu\sqrt{D\Delta}}{2eR(1+\nu)^2}\left(\tanh\frac{D}{2T} + \tanh\frac{\Delta}{2T}\right) \tag{40}$$

$$\delta J_{s4}(eV = 2\Delta) = \frac{\pi\nu^2\Delta}{2eR(1+\nu)^2}\tanh\frac{\Delta}{2T}. \tag{41}$$

The first two jumps to a great extent compensate each other, and for normal metals or superconductors above T_c the jump at $eV = 2D$ disappears, as was shown earlier [18].

If $T \neq 0$, a logarithmic singularity at $eV = D - \Delta$ appears:

$$J_{s3}(eV \approx D - \Delta) \approx \frac{\nu\sqrt{D\Delta}}{2eR(1+\nu)^2} W_2(D, \Delta). \tag{42}$$

Here

$$W_2(\Delta_1, \Delta_2) = \left|\tanh\frac{\Delta_1}{2T} - \tanh\frac{\Delta_2}{2T}\right| \ln\frac{4(\Delta_1 + \Delta_2)}{|eV - |\Delta_1 - \Delta_2||}. \tag{43}$$

The CVC depend on two dimensionless parameters characterizing the specific substance: ν and $\sigma(T) \equiv \Sigma(T)/\Delta_0$. According to the discussion in section 2, the dependence $\Sigma(T)$ is chosen to be of the BCS type, so its value at any given temperature T is determined by the parameter $\sigma_0 \equiv \Sigma_0/\Delta_0$, where $\Sigma_0 \equiv \Sigma(T = 0)$. The comparison of the results obtained with the molecular-field constant Σ and $\Sigma_{\mathrm{BCS}}(T)$ shows that the character of the difference is not qualitative. It reveals itself only in the vicinity of T_c, and is not crucial for the further presentation.

The family of dimensionless current amplitudes $i_s^1 \equiv I_s^1 eR/\Delta_0$, $j_s \equiv J_s eR/\Delta_0$, and the quasiparticle conductance $g_s \equiv \mathrm{d}j_s/\mathrm{d}x$ versus the dimensionless bias $x \equiv eV/\Delta_0$ are depicted in figure 1 for various FS degrees of 'dielectrization' at normalized temperatures $t \equiv T/T_{c0} = 0.4$. Here $T_{c0} = \gamma\Delta_0/\pi$ is the critical temperature of the CDW superconductor in the absence of the 'dielectrization' and $\gamma = 1.78\ldots$ is the Euler constant. The CVC discontinuities, which are too small to be seen at the chosen scale, are shown by the double arrows. One can see that the current and conductance magnitudes and the amplitudes of the singularities and jumps depend drastically on ν. Therefore, control over any external parameter affecting the electronic system (e.g., the applied pressure) may help one to observe the predicted peculiarities. It should be noted that dependence of the CVC features on ν has a twofold origin. First, ν enters the current amplitude explicitly. Second, it determines the actual values of T_c and Δ [15, 16], the latter also entering the expressions for currents. In figure 1, curve 1 corresponds to $T/T_c = 0.90$ and curve 2 to $T/T_c = 0.60$.

We have to note that the measured CVCs will differ from the ideal ones presented here. In particular, there always exists a certain spread of Δ magnitudes over the junction cross-section even for the single-crystal samples. One can easily show then that any logarithmic singularity will be smeared substantially to a smooth bump. Therefore, the minute logarithmic peaks of the type (43) will be almost averaged out, while their remnants can survive in the derivatives. Of course, the Riedel spikes of the type (36) will also be averaged. But they will be preserved as deformed features with finite amplitudes.

An interesting opportunity should be indicated for symmetrical junctions. Since the free energy of CDW superconductors does not depend on the sign of Σ [15, 20], it is reasonable to assume a possibility of Σ having different signs on the left- and right-hand sides of the symmetrical junction. The choice of the sign for the dielectric order parameter Σ may be associated with tiny random interactions not included in the Hamiltonian (1). Then the CVC of the quasiparticle current $J_s(V)$ for the *symmetrical* junction becomes *non-symmetrical!* Really, in this case the above-mentioned compensation between the components J_2 and J_3 and between J_6 and J_8 will no longer take place, and extra current components J_{s5} and

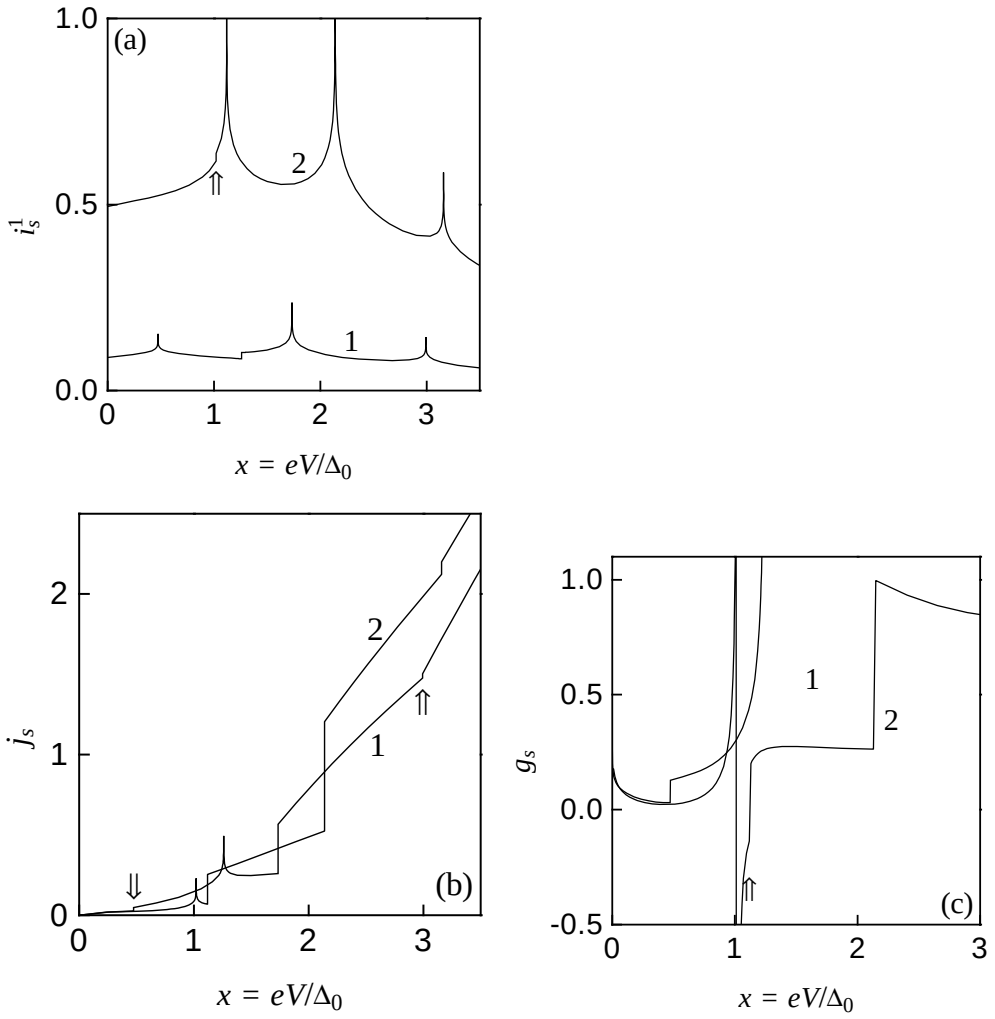

Figure 1. Comparison of current–voltage characteristics for symmetrical S–I–S tunnel junctions between CDW superconductors with different values of $\nu = N_{nd}(0)/N_d(0)$, where $N_{nd(d)}(0)$ is the electron density of states at the 'non-dielectrized' ('dielectrized') Fermi surface section: (a) the Josephson current $i_s^1 \equiv I_s^1 eR/\Delta_0$, (b) the quasiparticle current $j_s \equiv J_s eR/\Delta_0$, and (c) the quasiparticle conductance $g_s = \mathrm{d}j_s/\mathrm{d}x$. Here I_s^1 and J_s are the relevant current amplitudes, e is the elementary charge, R is the junction resistance in the normal state, Δ_0 is the superconducting gap at zero temperature $T = 0$ in the absence of the 'dielectrization', $x = eV/\Delta_0$, and V is the applied voltage. The calculation parameters are as follows: $\sigma_0 = 1.5$ is the value of $\sigma = \Sigma/\Delta_0$ at $T = 0$; $\Sigma(T)$ is the dielectric order parameter which obeys the BCS equation; $t = T/T_{c0} = 0.4$; $T_{c0} = \gamma\Delta_0/\pi$ is the superconducting critical temperature in the absence of the 'dielectrization'; and $\gamma = 1.7810\ldots$ is the Euler constant. Curves 1 and 2 correspond to $\nu = 0.5$ and 1. Double arrows indicate the positions of discontinuities which are small on the scale selected.

J_{s6} emerge in equation (20). Besides which, the component J_{s2} changes its sign. The full set of current components for such a junction with the broken symmetry is presented in appendix C. It is remarkable that

$$J_{s5,s6}(-V) = J_{s5,s6}(V) \tag{44}$$

contrary to the symmetry relation given in equation (32). Moreover, $J_s(V)$ depends now on the sign of Σ. The symmetry breaking leading to the listed radical consequences is analogous to that for magnetics [41]. Hereafter, we confine ourselves to the case in which $\Sigma > 0$ on the left-hand side and $\Sigma < 0$ on the right-hand side. For the reverse situation the CVC branches for positive and negative V simply change places.

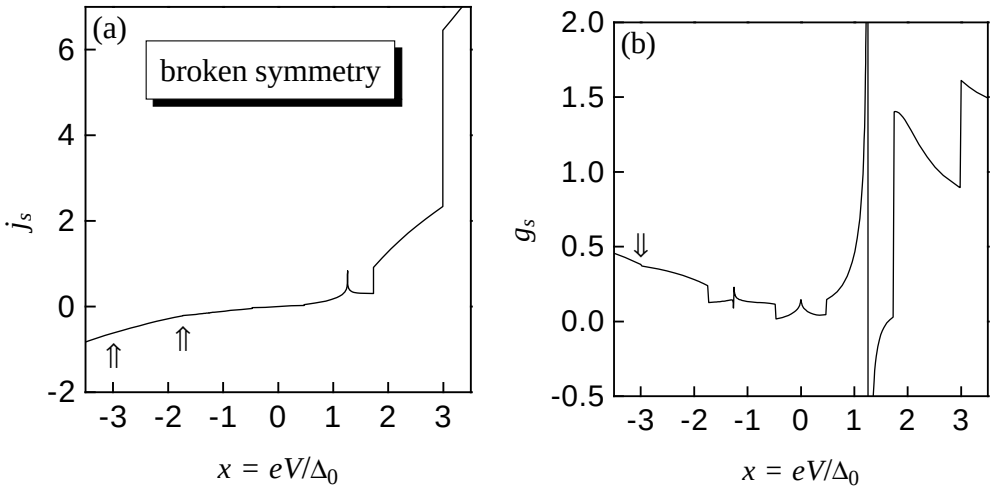

Figure 2. The dependences on x of (a) the quasiparticle current j_s and (b) the conductance g_s in the symmetrical tunnel junction with broken symmetry ($\Sigma > 0$ for the left-hand side and $\Sigma < 0$ for the right-hand side of the junction). The parameters are $\sigma_0 = 1.5$, $\nu = 0.5$, and $t = 0.4$.

An example of quasiparticle current and conductance dependences on the applied voltage for a symmetrical junction with broken symmetry is shown in figure 2. It is readily seen that the symmetrical S–I–S junctions made of partially 'dielectrized' superconductors may possess essentially non-symmetrical $j_s(x)$ and $g_s(x)$. The origin of the lack of symmetry will remain obscure for experimenters, because the input sample properties for each electrode would seem to be identical.

It should be stressed that the unconventional breaking of CVC symmetry is impossible for Josephson and interference currents between CDW superconductors, because the corresponding Green's function $\mathbf{F}_{is}$ is equal to zero.

For non-symmetrical S–I–S_{BCS} junctions it follows from appendix B that

$$I^1_{ns}(-V) = I^1_{ns}(V) \qquad J_{ns1,3}(-V) = -J_{ns1,3}(V). \tag{45}$$

But the term J_{ns2} has the non-conventional symmetry property, namely,

$$J_{ns2}(-V) = J_{ns2}(V). \tag{46}$$

Moreover, the CVC for $J_{ns2}(V)$ depends on the sign of Σ which is the factor in the relevant equation (cf. the case of broken symmetry for S–I–S junctions). This unusual dependence is a consequence of the fact that the 'interband' normal Green's function G_{is} (see equation (29)) inherent to excitonic (Peierls) insulators [3] appears in equation (A4) together with the standard (proportional to ω) normal Green's functions G_{nd} or G_d of superconductors. The dependence of the quasiparticle current $J_{ns}(V)$ on the sign of Σ is justified by calculations for the case of complete 'dielectrization' based on Bogoliubov's canonical transformation [28].

The analytical expressions for the currents I^1_{nsi} and J_{nsi} can be obtained only when $T = 0$. For finite temperatures the Riedel singularities of I^1_{nsi} are ($\Delta_{\rm BCS}$ is the gap of the BCS superconductor, eV is assumed to be positive)

$$I^1_{ns1}(eV \approx D + \Delta_{\rm BCS}) \approx \frac{\Delta\sqrt{\Delta_{\rm BCS}/D}}{4eR(1+\nu)} W_1(D, \Delta_{\rm BCS}) \tag{47}$$

$$I^1_{ns2}(eV \approx \Delta + \Delta_{\rm BCS}) \approx \frac{\nu\sqrt{\Delta\Delta_{\rm BCS}}}{4eR(1+\nu)} W_1(\Delta, \Delta_{\rm BCS}). \tag{48}$$

The non-zero-temperature features of these currents are similar to their symmetrical counterparts (37):

$$\delta I^1_{ns1}(eV = |D - \Delta_{\rm BCS}|) = \frac{\pi\Delta}{4eR(1+\nu)}\sqrt{\frac{\Delta_{\rm BCS}}{D}}\left|\tanh\frac{D}{2T} - \tanh\frac{\Delta_{\rm BCS}}{2T}\right| \tag{49}$$

$$\delta I^1_{ns2}(eV = |\Delta - \Delta_{\rm BCS}|) = \frac{\pi\nu\sqrt{\Delta\Delta_{\rm BCS}}}{4eR(1+\nu)}\left|\tanh\frac{\Delta}{2T} - \tanh\frac{\Delta_{\rm BCS}}{2T}\right|. \tag{50}$$

As results from the symmetry properties (45) and (46), the signs of the singularities and jumps for the quasiparticle current components are different for positive and negative voltages. Here we shall present them only for $V > 0$, the effects for $V < 0$ being the direct consequence of equations (45) and (46):

$$\delta J_{ns1}(eV = D + \Delta_{\rm BCS}) = \frac{\pi\sqrt{D\Delta_{\rm BCS}}}{4eR(1+\nu)}\left(\tanh\frac{D}{2T} + \tanh\frac{\Delta_{\rm BCS}}{2T}\right) \tag{51}$$

$$\delta J_{ns2}(eV = D + \Delta_{\rm BCS}) = \frac{\pi\Sigma}{4eR(1+\nu)}\sqrt{\frac{\Delta_{\rm BCS}}{D}}\left(\tanh\frac{D}{2T} + \tanh\frac{\Delta_{\rm BCS}}{2T}\right) \tag{52}$$

$$\delta J_{ns3}(eV = \Delta + \Delta_{\rm BCS}) = \frac{\pi\nu\sqrt{\Delta\Delta_{\rm BCS}}}{4eR(1+\nu)}\left(\tanh\frac{\Delta}{2T} + \tanh\frac{\Delta_{\rm BCS}}{2T}\right). \tag{53}$$

Provided that $\Sigma > 0$ and according to the symmetrical properties (45) and (46), the jumps δJ_{ns1} and δJ_{ns2} are added for $V > 0$, while for $V < 0$ they are subtracted, the situation being the inverse of this for $\Sigma < 0$. Thus, one CVC branch possesses a large jump at $eV = D + \Delta_{\rm BCS}$, while for another one the two contributions (51) and (52) almost compensate each other, because usually $\Sigma \gg \Delta$ and hence $D \approx \Sigma$ (see, e.g., [5, 8, 9]).

The opposite relationship takes place for logarithmic singularities of the currents $J_{ns1,ns2}$ at $eV = |D - \Delta_{\rm BCS}|$ emerging when $T \neq 0$:

$$J_{ns1}(eV \approx |D - \Delta_{\rm BCS}|) \approx \frac{\sqrt{D\Delta_{\rm BCS}}}{4eR(1+\nu)} W_2(D, \Delta_{\rm BCS}) \tag{54}$$

$$J_{ns2}(eV \approx |D - \Delta_{\rm BCS}|) \approx -\frac{\Sigma\sqrt{\Delta_{\rm BCS}/D}}{4eR(1+\nu)} W_2(D, \Delta_{\rm BCS}). \tag{55}$$

Here the approximate compensation of peaks is achieved for $V > 0$ when Σ is positive, whereas for $eV = -|D - \Delta_{\rm BCS}|$ the right-hand side of equation (55) changes its sign and the peaks enhance each other. The conventional singularity at $eV = |\Delta - \Delta_{\rm BCS}|$ is retained for CDW superconductors:

$$J_{ns3}(eV \approx |\Delta - \Delta_{\rm BCS}|) \approx \frac{\nu\sqrt{\Delta\Delta_{\rm BCS}}}{4eR(1+\nu)} W_2(\Delta, \Delta_{\rm BCS}). \tag{56}$$

The predicted features (47)–(56) are reproduced in numerical calculations. For the sake of definiteness, we assume that $\Sigma > 0$. In figure 3 the bias dependences of the normalized total currents $i^1_{ns} \equiv I^1_{ns}eR/\Delta_0$, $j_{ns} \equiv J_{ns}eR/\Delta_0$, and the conductances $g_{ns} \equiv {\rm d}j_{ns}/{\rm d}x$

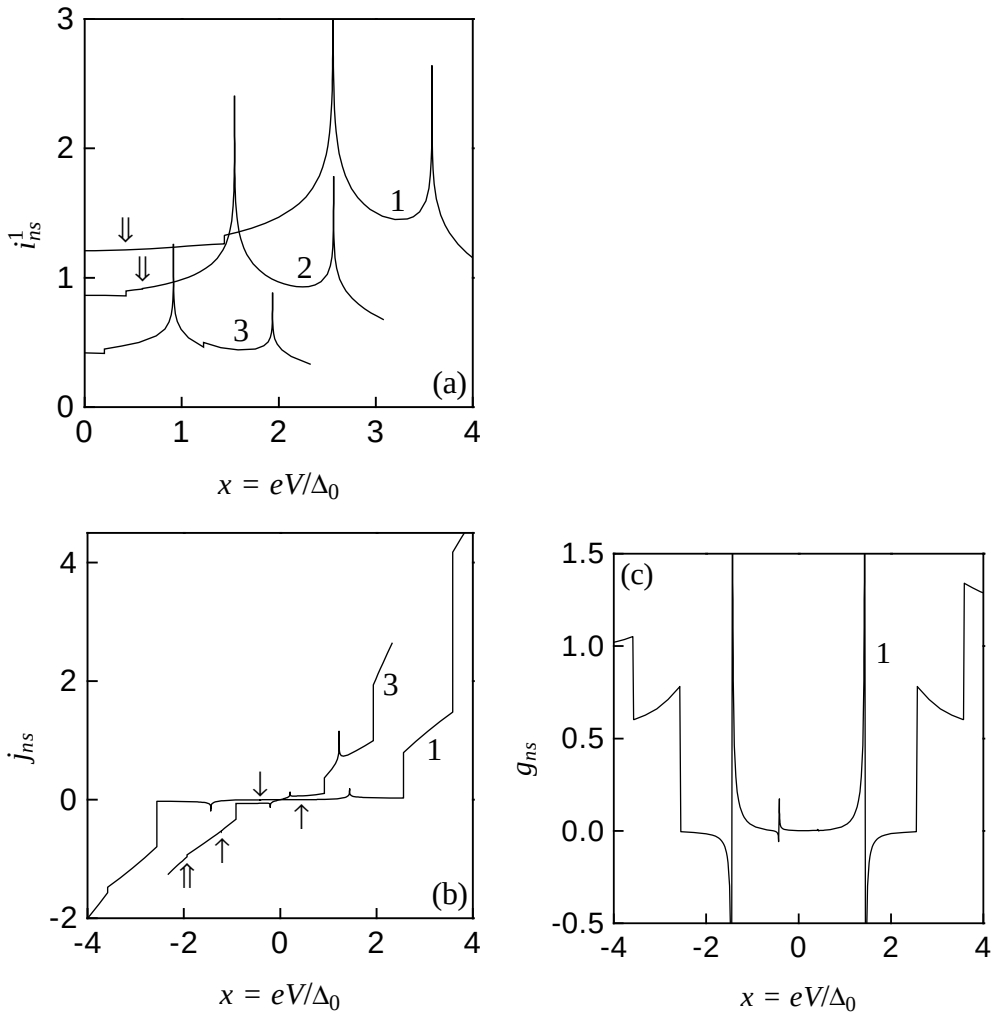

Figure 3. As figure 1, but for non-symmetrical S–I–S_{BCS} junctions, where S_{BCS} is an ordinary BCS superconductor with the gap Δ_{BCS}, and $\varepsilon_0 \equiv \Delta_{BCS}(T = 0)/\Delta_0 = 2, 1, 0.5$ (curves 1–3, respectively). $\sigma_0 = 1.5, \nu = 1, t = 0.4$. Single arrows indicate the positions of logarithmic singularities which are hardly seen on the scale selected.

are shown for various values of the ratio $\epsilon_0 \equiv \Delta_{BCS}(T = 0)/\Delta_0$. The small logarithmic singularities which are hard to detect because of their magnitudes are marked by single arrows. One can clearly see the absence of definite symmetry for quasiparticle currents, and, in particular, the difference in discontinuities for the two CVC branches.

The results obtained differ essentially from those of [28] dealing with the same subject. This is a direct consequence of the principal distinction between the problem formulations. Within the framework of the Bilbro–McMillan model [14] used here, we assume the zero value of the parameter $\mu(\boldsymbol{p})$ which describes the deviations of the FS nested sections from congruency, and is associated with the doping of the hypothetical material with the completely nested and hence completely 'dielectrized' FS [3]. Therefore, the chemical potential level in our model appears to be located inside the dielectric gap. But the system

remains a metal because a 'non-dielectrized' FS section is retained with the quasiparticle dispersion law $\xi_3(\boldsymbol{p})$. In the contrast, in [28] it is assumed that $\mu(\boldsymbol{p}) \neq 0$, and the FS 'non-dielectrized' section is absent altogether. Then the Fermi level lies outside the dielectric gap.

6. Discussion

The results presented above are of quite general character due to the phenomenological nature of our approach. The main obstacle which makes it difficult to obtain direct predictions for specific compounds is the absence of reliable parameter estimations, especially as regards the gapped FS fraction described by ν. The only exception is for the quasi-one-dimensional substance $NbSe_3$ [5]. Here superconductivity appears under pressure when the low-temperature CDW transition into the incommensurate state is suppressed, while the commensurate CDW distortion is still retained. The asymmetrical quasiparticle tunnelling conductivity was actually observed in planar Pb–I–$NbSe_3$ tunnel junctions [42], together with the insufficiency of the explanation [43] in the framework of the model [44] which takes into account the coupling energy in the transverse direction.

We would also like to call attention to the Andreev scattering experiments at the interface between Au and the non-superconducting Peierls insulator $K_{0.3}MoO_3$ which revealed the strong asymmetry of $g_{ns}^{-1}(x)$ [45].

The most intriguing issue is the validity of the concept outlined here for high-T_c oxides. It is worth noting that structural transitions in the overwhelming majority of high-T_c superconducting oxides occur at $T_d > T_c$. In some of them a dielectric gap (or at least its manifestations) in the FS parts is also observed. Thus, in $BaPb_{1-y}Bi_yO_3$ (BPB) for $y \geqslant 0.35$ the electron spectrum 'dielectrization' is complete, and superconductivity is absent, whereas for $y < 0.35$ the electrical conductivity has a metallic character and superconductivity appears at $T_c = T_c(y)$. Partial 'dielectrization' of the metallic state develops when $y \geqslant 0.15$; this is proved by a number of anomalies in the BPB properties [8, 15, 46]. But the most direct evidence for the existence of the order parameter Σ in BPB is provided by the light reflection spectra for the BPB ceramics [47]. The authors explain their results in terms of the frequency-dependent dielectric function $\epsilon(\omega)$ which does not have simple Drude-like character. In contrast, $\epsilon(\omega)$ involves a gap-type contribution, being the direct consequence of the Σ formation on the definite FS sections (a 'pseudogap'). The most probable source of the electron spectrum 'dielectrization' in BPB is the emergence of CDW induced by the alternation of the Bi^{3+} and Bi^{5+} states [8, 48].

For the BPB oxide with $T_c^{\max} = T_c(y = 0.25) \approx 13$ K, the values of Σ extracted from the thermodynamic and resistive data are estimated approximately as $\Sigma \geqslant 50$–100 K [8]. Experimental data on the peculiarities of the quasiparticle currents through BPB-based junctions are also available. According to [49], the gap-edge voltage grows with increasing y and reaches a level $V_{\rm up}$ at $y \geqslant 0.2$ for which the ratio $V_{\rm up}/T_c$ is equal to the BCS weak-coupling value $\Delta(T = 0)/T_c = \pi/\gamma$ [1]. On the other hand, in BPB with $y = 0.25$, gap features appear in the bias range 60–100 K of tunnel characteristics, depending on the sample and the estimation method [50]. However, the T_c-values in [49, 50] virtually coincide. The results of [50] can be understood on the basis of our theory. In this case the smaller gap $\Delta_{\min}$ is likely to be indistinguishable against the background of the larger one $\Delta_{\max}$. This could be associated with a smearing of the anomaly corresponding to the dielectric gap $\Sigma \equiv \Delta_{\max}$ due to the averaging of the contributions to the total current $J(V)$ from areas with different values of Σ. A possible source of the Σ magnitude spread may be the chemical inhomogeneities of the grain boundaries mentioned above [8, 51].

Nevertheless, the question is far from receiving a final solution.

The FS of the solid solutions $Ba_{1-y}K_yBiO_3$ (BKB), like in the BPB case, contains nested sections for arbitrary y that lead to CDW formation [52, 53]. The possibility of the existence of Σ in the superconducting y-compositions can be inferred from the observed positive curvature [54] of the dependence of the upper critical magnetic field H_{c2} on T near T_c common to partially 'dielectrized' superconductors [15] (see also the discussion in reference [55]). The light reflection spectra [56] for the superconducting single crystals $Ba_{0.6}K_{0.4}BiO_3$ confirm this point of view: the ac conductance reveals the same finite-gap non-Drude contribution as for BPB [47]. Direct evidence that incommensurate CDW modulations do exist in superconducting BKB ($x > 0.37$) was obtained in electron diffraction experiments [57]. In tunnel CVC of superconducting BKB samples one gap feature was revealed [58]. In order to reconcile these data with the evidence for the Σ and Δ coexistence, one may adopt the hypothesis [56] of the percolative nature of the non-cubic semiconducting BKB phase in bulk superconducting crystals.

Now let us turn to high-T_c cuprate oxides. The most thoroughly studied among them are the 214 and 123 systems with $T_c \approx 40$ K and 90 K, respectively. Electron band-structure calculations show that in La_2CuO_4-based layered perovskites and in the $YBa_2Cu_3O_{7-y}$ superconductor there are congruent FS sections [59]. The T–y phase diagrams of these compounds, where y denotes the content of the doping metal (Ba, Ca, Sr) for the 214 system or the oxygen concentration for the 123 system, involve various structural transitions, even in a close neighbourhood of T_c. As was mentioned in the introduction, the CDW reflections were *directly* observed by means of electron diffraction for the compounds $La_{2-x}[Ba(Sr)]_xCuO_4$ and $La_{1.880-y}Nd_ySr_{0.120}CuO_4$ [11], and by the STM technique for Cu–O chains in $YBa_2Cu_3O_{7-y}$ [12].

Structural phase transitions take place also in Bi-based high-T_c materials. Thus, ultrasound attenuation measurements [60] show that in $Bi_2Sr_2CaCu_2O_8$ with $T_c = 84$ K there are structural anomalies at $T_d = 95$ K and 250 K, while in Bi–Sr–Ca–Cu–Pb–O with $T_c \approx 107$ K the anomalies are at $T_d = 130$ K and 250 K. The corresponding dielectric gap $|\Sigma|$ seems to have already been observed in the angle-resolved photoemission experiments [25] on underdoped samples of oxygen-depleted $Bi_2Sr_2CaCu_2O_{8+\delta}$ ($T_c \approx 67$ K) near the $(\pi, 0)$ point in the Brillouin zone.

It should be noted that the so-called pseudogap state in various underdoped high-T_c oxides—the subject of the recent concentrated experimental attack [61]—may originate from the dielectric gapping (in the spirit of the earlier approach [10]) rather than from a superconducting pairing of the still unclarified nature. Thus our suggestion can explain the genesis of the almost T-independent 'superconducting gap' above T_c in the underdoped samples of $Bi_2Sr_2Ca_{1-x}Dy_xCu_2O_{8+\delta}$ [62].

Tunnel and point-contact spectroscopies, as well as STM, have shown the high-T_c superconductor quasiparticle CVCs to deviate substantially from those calculated in the framework of the BCS theory. Unfortunately, the gap values extracted from the differential conductivities $G^{\rm diff}_{s(ns)} = {\rm d}J_{s(ns)}/{\rm d}V$ differ for the same substance when measured by various groups [63, 64]. This undesirable situation may be due not only to the poor quality of the samples and junctions, but also to intrinsic phenomena in oxides connected to their thermal history [8].

The main unusual properties that are often observed for different cuprates are as follows. A two-gap structure is revealed in point-contact CVC of $La_{2-y}Sr_yCuO_4$ [63], in tunnel CVC of $YBa_2Cu_3O_{7-y}$ [65], in point contacts of $YBa_2(Cu_{1-y}Zn_y)_3O_7$ [66], and in break junctions of $Yb(Y)Ba_2Cu_3O_{7-y}$ [67]. With the help of the STM technique, the complex gap-like structure of $G^{\rm diff}_{ns}(V)$ was discovered for $Bi_2Sr_2CaCu_2O_y$ [68]. Two kinds of gap peculiarity

at $eV \approx 21$ meV and 51 meV were revealed in $HgBa_2Ca_2Cu_3O_{8-y}$ with $T_c \approx 132$ K, both in STM and in point-contact experiments [69]. We think that in view of the facts presented above and concerning the existence of the structural transitions in cuprates, our theory can be applied to explain the gap properties of tunnel and point-contact characteristics. In doing this, the larger gap should be identified with $D = (\Delta^2 + \Sigma^2)^{1/2}$. This assumption is supported by the tunnel measurements on the symmetrical sandwich involving Bi–Sr–Ca–Cu–O with $T_c \approx 75$ K [70]. There the larger gap singularity of $G_s^{\rm diff}$ weakly depends on T up to T_c and disappears above T_c. Such a behaviour can be explained if the curve $\Sigma(T)$ has a non-BCS form close to rectangular (this is approximately true when the ratio $\Sigma(0)/T_d$ is well above the BCS value π/γ), and T_d is slightly higher than T_c.

The other feature inherent to high-T_c oxides is the asymmetry of the CVC with respect to the voltage polarity. The types of phenomenon may be different; e.g., in the STM measurements of $J_{ns}(V)$ for $Bi_2Sr_2CaCu_2O_{8+y}$ a dip was observed in $G_{ns}^{\rm diff}$ only for $V < 0$ [71]. When the Bi-based ceramics constituted a two-phase mixture with $T_c \approx 85$ K and 110 K, the tunnel measurements revealed a similar dependence of the CVC on the sign of V [72]. Asymmetric CVCs were observed for $YBa_2Cu_3O_{7-y}$ by STM [12, 73]. Finally, point-contact and STM spectra for $HgBa_2Ca_2Cu_3O_{8-y}$ also showed an asymmetric character [69]. The observed dependences of the $J_{ns}(V)$ form on the voltage polarity may be considered as a direct consequence of our equations (B7*b*) if one takes into account the existing electron spectrum 'dielectrization' of cuprates.

To summarize, we should stress that it is impossible now to compare our theory for Josephson currents $I^1(V)$ with experiment, because Riedel singularities of the CVC for junctions involving CDW superconductors have not yet been investigated. All the same, the unconventional properties of $J(V)$ observed for many substances (see above) make parallel measurements of $I^1(V)$ very interesting.

Acknowledgments

We are grateful to I Bozović (Palo Alto), C H Du (Edinburgh), F Gervais and R P S M Lobo (Orleans), Z Ivanov (Göteborg), A Sinchenko (Moscow), and T Timusk (Hamilton) for providing us with their important experimental data. This work was supported, in part, by the INTAS Grant No 94-3862 and the Ukrainian State Foundation for Fundamental Research (Grant 2.4/100).

Appendix A

The expressions for the CVC of $I_i^{1,2}(V)$ and $J_i(V)$ in the general case of a junction between two different partially 'dielectrized' superconductors are (to be compared with [29]) as follows. We use the notation $F'_{ij} \equiv F_{i'j'}$ and $G'_{ij} \equiv G_{i'j'}$.

For Josephson ($j = 1$) and interference ($j = 2$) currents

$$\begin{aligned} I_1^j &= \varphi_j(F_{11}^+, F'_{11}) \qquad I_2^j = \nu'\varphi_j(F_{11}^+, F'_{33}) \\ I_3^j &= \nu\varphi_j(F_{33}^+, F'_{11}) \qquad I_4^j = \nu\nu'\varphi_j(F_{33}^+, F'_{33}) \end{aligned} \tag{A1}$$

$$\varphi_1(F_{ij}^+, F'_{mn}) = \frac{1}{2\pi^3 eR(1+\nu)(1+\nu')}\,\mathrm{Re}\left\{\mathrm{i}\int_{-\infty}^{\infty}\mathrm{d}\omega\int_{-\infty}^{\infty}\mathrm{d}\omega'\,\frac{\mathrm{Im}[F_{ij}^+(\omega)F'_{mn}(\omega')]}{\omega+\omega'+eV+\mathrm{i}0}\right\} \tag{A2}$$

$$\varphi_2(F^+_{ij}, F'_{mn}) = -\frac{1}{2\pi^3 eR(1+\nu)(1+\nu')}\,\mathrm{Re}\left\{\int_{-\infty}^{\infty}\mathrm{d}\omega\int_{-\infty}^{\infty}\mathrm{d}\omega'\;\frac{\mathrm{Im}[F^+_{ij}(\omega)F'_{mn}(\omega')]}{\omega+\omega'+eV+\mathrm{i}0}\right\}. \tag{A3}$$

For a quasiparticle current

$$\begin{aligned} &J_1=\varphi_3(G_{11},G'_{11}) \qquad J_2=\varphi_3(G_{11},G'_{12}) \qquad J_3=\varphi_3(G_{12},G'_{11})\\ &J_4=\varphi_3(G_{12},G'_{12}) \qquad J_5=\nu'\varphi_3(G_{11},G'_{33}) \qquad J_6=\nu'\varphi_3(G_{12},G'_{33})\\ &J_7=\nu\varphi_3(G_{33},G'_{11}) \qquad J_8=\nu\varphi_3(G_{33},G'_{12}) \qquad J_9=\nu\nu'\varphi_3(G_{33},G'_{33}) \end{aligned} \tag{A4}$$

$$\varphi_3(G_{ij}, G'_{mn}) = \frac{1}{2\pi^3 eR(1+\nu)(1+\nu')}\,\mathrm{Re}\left\{\int_{-\infty}^{\infty}\mathrm{d}\omega\int_{-\infty}^{\infty}\mathrm{d}\omega'\;\frac{\mathrm{Im}[G_{ij}(\omega)G'_{mn}(\omega')]}{\omega-\omega'-eV+\mathrm{i}0}\right\}. \tag{A5}$$

Appendix B

We introduce auxiliary functions:

$$N_1(\omega,\Delta)=\theta(\Delta-|\omega|)(\Delta^2-\omega^2)^{-1/2} \qquad N_2(\omega,\Delta)=\theta(|\omega|-\Delta)(\omega^2-\Delta^2)^{-1/2} \tag{B1}$$

where $\theta(x)$ is the Heaviside theta-function, and use the following notation:

$$\begin{aligned}\Phi_1(\Delta_1,\Delta_2) &= \frac{\Delta^2}{2eR(1+\nu)^2}\int_{-\infty}^{\infty}\mathrm{d}\omega\;\tanh\frac{|\omega|}{2T}\\ &\quad\times[N_1(\omega-eV,\Delta_1)N_2(\omega,\Delta_2)+N_2(\omega,\Delta_1)N_1(\omega+eV,\Delta_2)]\end{aligned} \tag{B2}$$

$$\begin{aligned}\Phi_2(\Delta_1,\Delta_2) &= -\frac{\Delta^2}{2eR(1+\nu)^2}\int_{-\infty}^{\infty}\mathrm{d}\omega\left(\tanh\frac{\omega-eV}{2T}-\tanh\frac{\omega}{2T}\right)\\ &\quad\times\mathrm{sgn}(\omega-eV)\,\mathrm{sgn}\,\omega\,N_2(\omega-eV,\Delta_1)N_2(\omega,\Delta_2)\end{aligned} \tag{B3}$$

$$\begin{aligned}\Phi_3(\Delta_1,\Delta_2) &= -\frac{1}{2eR(1+\nu)^2}\int_{-\infty}^{\infty}\mathrm{d}\omega\left(\tanh\frac{\omega-eV}{2T}-\tanh\frac{\omega}{2T}\right)\\ &\quad\times|\omega-eV|\,|\omega|\,N_2(\omega-eV,\Delta_2)N_2(\omega,\Delta_1)\end{aligned} \tag{B4}$$

$$\begin{aligned}\Phi_4(\Delta_1,\Delta_2) &= \frac{1}{2eR(1+\nu)}\int_{-\infty}^{\infty}\mathrm{d}\omega\left(\tanh\frac{\omega-eV}{2T}-\tanh\frac{\omega}{2T}\right)\\ &\quad\times\mathrm{sgn}(\omega-eV)\,|\omega|\,N_2(\omega-eV,\Delta_2)N_2(\omega,\Delta_1).\end{aligned} \tag{B5}$$

Then the amplitudes of the various current components obtained from the equations of appendix A, with the help of the formulas (25)–(31), in the symmetrical case take the form

$$I^m_{s1}=\Phi_m(D,D) \qquad I^m_{s2}=2\nu\Phi_m(D,\Delta) \qquad I^m_{s3}=\nu^2\Phi_m(\Delta,\Delta) \qquad (m=1,2) \tag{B6a}$$

$$\begin{aligned} &J_{s1}=\Phi_3(D,D) \qquad J_{s2}=(\Sigma/\Delta)^2\Phi_2(D,D)\\ &J_{s3}=2\nu\Phi_3(D,\Delta) \qquad J_{s4}=\nu^2\Phi_3(\Delta,\Delta). \end{aligned} \tag{B6b}$$

In the non-symmetrical case we obtain in a similar way

$$\begin{aligned} &I^m_{ns1}=(1+\nu)\Delta_{\mathrm{BCS}}\Delta^{-1}\Phi_m(D,\Delta_{\mathrm{BCS}})\\ &I^m_{ns2}=\nu(1+\nu)\Delta_{\mathrm{BCS}}\Delta^{-1}\Phi_m(\Delta,\Delta_{\mathrm{BCS}}) \end{aligned} \qquad (m=1,2) \tag{B7a}$$

$$\begin{aligned} &J_{ns1}=(1+\nu)\Phi_3(D,\Delta_{\mathrm{BCS}})\\ &J_{ns2}=\Sigma\Phi_4(\Delta_{\mathrm{BCS}},D)\\ &J_{ns3}=\nu(1+\nu)\Phi_3(\Delta,\Delta_{\mathrm{BCS}}). \end{aligned} \tag{B7b}$$

For both cases $m=1$ corresponds to Josephson amplitudes, and $m=2$ to interference current amplitudes.

Appendix C

In the case of broken symmetry for the symmetrical junction when $\Sigma > 0$ on the left-hand side and $\Sigma < 0$ on the right-hand side of the junction, the components of the quasiparticle current have the form

$$\begin{aligned} J_{s1} &= \Phi_3(D, D) & J_{s2} &= -(\Sigma/\Delta)^2\Phi_2(D, D) \\ J_{s3} &= 2\nu\Phi_3(D, \Delta) & J_{s4} &= \nu^2\Phi_3(\Delta, \Delta) \\ J_{s5} &= 2|\Sigma|\Phi_4(D, D)/(1+\nu) & J_{s6} &= 2\nu|\Sigma|\Phi_4(\Delta, D)/(1+\nu). \end{aligned} \tag{C1}$$

References

[1] Abrikosov A A, Gor'kov L P and Dzyaloshinskii I E 1963 *Methods of Quantum Field Theory in Statistical Physics* (Englewood Cliffs, NJ: Prentice-Hall)
[2] Halperin B I and Rice T M 1968 *Solid State Physics* vol 21 (New York: Academic) p 115
[3] Kopaev Yu V 1975 *Trudy Fiz. Inst. Akad. Nauk SSSR* **86** 3
[4] Bucher B, Steiner P and Wachter P 1991 *Phys. Rev. Lett.* **67** 2717
Wachter P, Jung A and Steiner P 1995 *Phys. Rev.* B **51** 5542
[5] Grüner G and Zettl A 1985 *Phys. Rep.* **119** 117
Grüner G 1988 *Rev. Mod. Phys.* **60** 1129
[6] Thorne R 1996 *Phys. Today* **49** (5) 42
[7] Grüner G 1994 *Rev. Mod. Phys.* **66** 1
[8] Gabovich A M, Moiseev D P and Shpigel A S 1982 *Sov. Phys.–JETP* **56** 795
Gabovich A M, Moiseev D P and Shpigel A S 1982 *J. Phys. C: Solid State Phys.* **15** L569
Gabovich A M, Moiseev D P, Prokopovich L V, Uvarova S K and Yachmenev V E 1984 *Sov. Phys.–JETP* **59** 1006
Gabovich A M and Moiseev D P 1986 *Sov. Phys.–Usp.* **29** 1135
[9] Pan V M, Prokhorov V G and Shpigel A S 1984 *Metal Physics of Superconductors* (Kiev: Naukova Dumka) (in Russian)
[10] Gabovich A M 1992 *High-T_c Superconductivity Experiment and Theory* ed A S Davydov and V M Loktev (Berlin: Springer) p 161
[11] Koyama Y, Wakabayashi Y, Ito K and Inoue Y 1995 *Phys. Rev.* B **51** 9045
[12] Edwards H L, Derro D J, Barr A L, Markert J T and de Lozanne A L 1995 *Phys. Rev. Lett.* **75** 1387
[13] Rice T M and Scott G K 1975 *Phys. Rev. Lett.* **35** 120
Markiewicz R S 1990 *Physica* C **169** 63
Markiewicz R S 1994 *Physica* C **228** 227
Markiewicz R S 1991 *Int. J. Mod. Phys.* B **5** 2037
Abrikosov A A, Campuzano J C and Gofron K 1993 *Physica* C **214** 73
[14] Bilbro G and McMillan W L 1976 *Phys. Rev.* B **14** 1887
[15] Gabovich A M and Shpigel A S 1983 *J. Low Temp. Phys.* **51** 581
Gabovich A M and Shpigel A S 1984 *J. Phys. F: Met. Phys.* **14** 1031
Gabovich A M and Shpigel A S 1988 *Phys. Rev.* B **38** 297
Gabovich A M, Gerber A S and Shpigel A S 1987 *Phys. Status Solidi* b **141** 575
[16] Voitenko A I, Gabovich A M, Moiseev D P and Shpigel A S 1989 *3rd USSR Symp. on Inhomogeneous Electron States (Novosibirsk)* abstracts, p 198 (in Russian)
Gabovich A M, Moiseev D P, Shpigel A S and Voitenko A I 1990 *Phys. Status Solidi* b **161** 293
[17] Kulik I O and Yanson I K 1970 *The Josephson Effect in Superconducting Tunnel Structures* (Moscow: Nauka) (in Russian)
[18] Gabovich A M 1993 *Low Temp. Phys.* **19** 779
Gabovich A M and Voitenko A I 1995 *Phys. Rev.* B **52** 7437
[19] de Gennes P G 1966 *Superconductivity of Metals and Alloys* (New York: Benjamin)
[20] Gabovich A M, Pashitskii E A and Shpigel A S 1979 *Sov. Phys.–JETP* **50** 583
[21] Gabovich A M and Pashitskii E A 1975 *Fiz. Tverd. Tela* **17** 1584
[22] Gabovich A M, Pashitskii E A and Shpigel A S 1976 *Sov. Phys.–Solid State* **18** 1911
[23] Pashitskii E A 1995 *JETP Lett.* **61** 275
Pashitskii E A and Pentegov V I 1996 *Pis. Zh. Eksp. Teor. Fiz.* **63** 553

Pashitskii E A, Pentegov V I and Semenov A V 1996 *Low Temp. Phys.* **22** 367
[24] Shen Z-X, Dessau D S, Wells B O, King D M, Spicer W E, Arko A J, Marshall D, Lombardo L W, Kapitulnik A, Dickinson P, Doniach S, Di Carlo J, Loeser A G and Park C H 1993 *Phys. Rev. Lett.* **70** 1553
Ding H, Campuzano J C, Bellman A F, Yokoya T, Norman M R, Randeira M, Takahashi T, Katayama-Yoshida H, Mochiki T, Kadowaki K and Jennings G 1995 *Phys. Rev. Lett.* **74** 2784
[25] Marshall D S, Dessau D S, Loeser A G, Park C-H, Matsuura A Y, Eckstein J N, Bozović I, Fournier P, Kapitulnik A, Spicer W E and Shen Z-X 1996 *Phys. Rev. Lett.* **76** 4841
[26] Geilikman B T and Kresin V Z 1972 *Transport and Nonstationary in Superconductors* (Moscow: Nauka) (in Russian)
[27] Gabovich A M 1992 *Sov. J. Low Temp. Phys.* **18** 490
Gabovich A M 1993 *Int. J. Mod. Phys.* B **7** 3927
[28] Ismagilov A M and Kopaev Yu V 1989 *Sov. Phys.–JETP* **69** 846
[29] Larkin A I and Ovchinnikov Yu N 1966 *Sov. Phys.–JETP* **24** 1035
[30] Fröhlich H 1954 *Proc. R. Soc.* A **223** 296
Lee P A, Rice T M and Anderson P W 1974 *Solid State Commun.* **14** 703
[31] Guseinov R R and Keldysh L V 1972 *Zh. Eksp. Teor. Fiz.* **63** 2255
[32] Gorbatsevich A A and Kopaev Yu V 1987 *Superconductivity, Superdiamagnetism, Superfluidity* (Moscow: Mir) p 175
[33] Volkov B A and Kopaev Yu V 1978 *Sov. Phys.–JETP* **27** 7
[34] Elesin V F 1970 *Zh. Eksp. Teor. Fiz.* **59** 602
Galitskii V M and Elesin V F 1986 *Resonance Interaction of Electromagnetic Fields with Semiconductors* (Moscow: Energoatomizdat)
[35] Artemenko S N and Volkov A F 1984 *Zh. Eksp. Teor. Fiz.* **87** 691
[36] Blonder G E, Tinkham M and Klapwijk T M 1982 *Phys. Rev.* B **25** 4515
[37] Visscher M I and Bauer G E W 1996 *Phys. Rev.* B **54** 2798
Tanaka Y, Visscher M I, Rejaei B and Bauer G E W 1996 *Solid State Commun.* **100** 37
[38] Andreev A F 1964 *Sov. Phys.–JETP* **19** 1228
[39] Kasatkin A L and Pashitskii E A 1984 *Fiz. Nizhk. Temp.* **10** 1222
Kasatkin A L and Pashitskii E A 1985 *Fiz. Tverd. Tela* **27** 2417
[40] Zorin A B, Kulik I O, Likharev K K and Schrieffer J R 1979 *Sov. J. Low Temp. Phys.* **5** 537
[41] White R and Geballe T 1979 *Long Range Order in Solids* (New York: Academic)
[42] Sorbier J P, Tortel H, Monceau P and Levy F 1996 *Phys. Rev. Lett.* **76** 676
[43] Huang X and Maki K 1989 *Phys. Rev.* B **40** 2575
Huang X and Maki K 1992 *Phys. Rev.* B **46** 162
[44] Yamaji K 1982 *J. Phys. Soc. Japan* **51** 2787
[45] Sinchenko A A, Latyshev Yu I, Zybtsev S G, Gorlova I G and Monceau P 1996 *Pis. Zh. Eksp. Teor. Fiz.* **64** 259
[46] Hashimoto T, Hirazawa R, Yoshida T, Yonemura Y, Mizusaki J and Tagawa H 1995 *Phys. Rev.* B **51** 576
[47] Tajima S, Uchida S, Masaki A, Takagi H, Kitazawa K and Tanaka S 1985 *Phys. Rev.* B **32** 6302
[48] Lobo R P S M and Gervais F 1995 *Phys. Rev.* B **52** 13 294
Lobo R P S M and Gervais F 1996 *Solid State Commun.* **98** 61
[49] Ekino T and Akimitsu J 1989 *J. Phys. Soc. Japan* **58** 2135
[50] Suzuki M, Komoriota K, Nakano H and Rinderer L 1990 *J. Less-Common Met.* **164+165** 1579
[51] Kuznetsov A V, Protasov E A and Stepankin V N 1987 *Superconductivity in* $BaPb_{1-x}Bi_xO_3$ (Moscow: Energoatomizdat) (in Russian)
[52] Hahn U, Vielsack G and Weber W 1994 *Phys. Rev.* B **49** 15 936
[53] Mosley W D, Dykes J W, Shelton R N, Sterne P A and Howell R H 1994 *Phys. Rev. Lett.* **73** 1271
[54] Affronte M, Marcus J, Escribe-Filippini C, Sulpice A, Rakoto H, Broto J M, Ousset J C, Askenazy S A and Jansen A G M 1994 *Phys. Rev.* B **49** 3502
Gantmakher V F, Klinkova L A, Barkovskii N V, Tsydynzhapov G E, Wiegers S and Geim A K 1996 *Phys. Rev.* B **54** 6133
[55] Anshukova N V, Golovashkin A I, Ivanova L I, Malyuchkov O T and Rusakov A P 1995 *Zh. Eksp. Teor. Fiz.* **108** 2132
[56] Puchkov A V, Timusk T, Mosley W D and Shelton R N 1994 *Phys. Rev.* B **50** 4144
[57] Verwerft M, Van Tendeloo G, Hinks D G, Dabrowski B, Richards D R, Mitchell A W, Marx D T, Pei S and Jorgensen J D 1991 *Phys. Rev.* B **44** 9547
Du C-H, Hatton P D, Tang H Y and Wu M K 1994 *J. Phys.: Condens. Matter* **6** L575
Du C-H and Hatton P D 1995 *Europhys. Lett.* **31** 145

[58] Morales F, Escudero R, Hinks D G and Zheng Y 1990 *Physica* C **169** 294
[59] Pickett W E 1989 *Rev. Mod. Phys.* **61** 433 (erratum 1989 **61** 749)
[60] Wang Y, Shen H, Zhu M and Wu J 1990 *Solid State Commun.* **76** 1273
[61] Levi B G 1996 *Phys. Today* **49** (6) 17
Puchkov A V, Basov D N and Timusk T 1996 *J. Phys.: Condens. Matter* **8** 10 049
[62] Harris J M, Loeser A G, Marshall D S, Schabel M C, Shen Z-X, Eckstein J N and Bozović I 1996 *Phys. Rev.* B **54** 15 665
[63] Yanson I K 1991 *Sov. J. Low Temp. Phys.* **17** 143
[64] Hasegawa T, Ikuta H and Kitazawa K 1992 *Physical Properties of High Temperature Superconductors III* ed D M Ginsberg (Singapore: World Scientific) p 525
[65] Geerk J, Xi X X and Linker G 1989 *Z. Phys.* B **73** 329
Geerk J, Linker G, Meyer O, Li Q, Wang R-L and Xi X X 1989 *Physica* C **162–164** 837
[66] Akimenko A I, Goll G, Yanson I K, von Löhneysen H, Ahrens R, Wolf T and Wühl H 1991 *3rd USSR Symp. on High Temperature Superconductivity (Kharkov)* abstracts, part II, p 85 (in Russian)
[67] Aminov B A, Hein M A, Müller G, Piel H, Wehler D, Ponomarev Ya G, Rosner K and Winczer K 1994 *J. Supercond.* **7** 361
[68] Barbiellini B, Fischer Ø, Peter M, Renner C and Weger M 1994 *Physica* C **220** 55
[69] Jeong G T, Kye J I, Chun S H, Lee S, Lee S I and Khim Z G 1994 *Phys. Rev.* B **49** 15 416
[70] Walsh T, Moreland J, Ono R H and Kalkur T S 1991 *Phys. Rev.* B **43** 11 492
[71] Renner C and Fischer Ø 1995 *Phys. Rev.* B **51** 9208
[72] Kussmaul A, Moodera J S, Roesler G M Jr and Tedrov P M 1990 *Phys. Rev.* B **41** 842
[73] Kubatkin S E, Tzalenchuk A Ya, Ivanov Z G, Delsing P, Shekhter R I and Claeson T 1996 *JETP Lett.* **63** 126